JOURNAL OF THERMOPHYSICS AND HEAT TRANSFER
Vol. 10, No. 1, January–March 1996

# Predictions of Radiative Transfer in Two-Dimensional Nonhomogeneous Participating Cylindrical Media

Jian-Min Zhang* and William H. Sutton†
*University of Oklahoma, Norman, Oklahoma 73019*

**The surface-integral form of radiative transfer equation is formulated to accommodate nonhomogeneous radiative properties for a multidimensional participating medium. A straightforward numerical quadrature scheme is then applied to solve the equation of transfer for test cases of radiation in an absorbing, emitting, anisotropic-scattering, two-dimensional cylindrical medium with space-dependent radiative properties. To illustrate the effectiveness and accuracy of the approach, the product-integration method (PIM) is also used as a benchmark comparison in the numerical analysis. It is shown that consistent numerical predictions are obtainable by both schemes for the cases considered, whereas the computational efforts for the current method are much less than those required by the PIM.**

## Nomenclature

$A$ = area of enclosure wall
$a_k$ = scattering phase function coefficients
$d$ = geometric distance
$G$ = incident radiation, defined in Eq. (4)
$I$ = radiation intensity
$L$ = axial length of cylindrical enclosure
$M$ = number of zeros for Gauss quadrature
$N$ = number of grid points
$\hat{n}$ = unit direction vector
$P_k$ = Legendre polynomials, $k$th order
$q$ = component of radiative heat flux
$\boldsymbol{q}$ = radiative heat flux vector, defined in Eq. (5)
$R$ = radius of cylindrical enclosure
$r$ = radial coordinate
$S$ = radiation source function
$s$ = position or a path along which a radiation beam travels
$w_m$ = weight factor for Gauss quadrature for $m$th zero point
$x_m$ = abscissas for Gauss quadrature for $m$th zero point
$z$ = axial coordinate
$\beta$ = extinction coefficient
$\varepsilon$ = emissivity
$\Theta$ = scattering angle
$\Lambda$ = integrand, defined in Eq. (24)
$\rho$ = reflectivity
$\tau$ = optical length
$\Phi$ = scattering phase function
$\phi$ = azimuth angle
$\Omega$ = solid angle
$\hat{\Omega}$ = unit direction vector of radiation intensity
$\omega$ = single scattering albedo

*Subscripts*
$b$ = blackbody
out = outgoing heat flux from the medium into boundary
$r$ = quantity in $r$ direction
$s$ = indicates the coordinates being a function of $s$
$z$ = quantity in $z$ direction

*Superscripts*
$d$ = diffuse
$s$ = specular
$*$ = quantity on wall surface

## Introduction

THE development of general and accurate solution methods to the equation of radiative transfer remains a robust area in the study of heat transfer. Numerous modeling techniques[1–11] have appeared in recent years that show good promise in at least one of the following aspects, such as being applicable to multidimensional and complex geometries, working well with nonuniform radiative properties in space, being computationally efficient in solving combined modes of heat transfer, and incorporating anisotropic scattering and spectral properties. Since the radiation in a participating medium can be exactly modeled by an integral form of transfer equation,[10–14] which may directly give the heat flux or divergence of heat flux over the entire medium, several numerical approaches, including the point collocation method[2,3] and the product-integration method (PIM),[10,11] have been developed to solve the integral form of radiative transfer equation with high accuracy and moderate computation efficiency.

Recently, the authors proposed an equivalent, alternative, surface-related integral equation of transfer based on radiative source approximation.[15] In this integral equation method the incident radiation and radiative heat flux are formulated by their definitions and the expression for intensity is obtained by direct line integration with source interpolation. Thus, all of the effects of the entering intensity on boundary, emission source, and in-scattering in medium can be accounted for in double-integral(s) with respect to bounding surface(s). To differentiate between the previous integral equation of transfer[10–14] and this modeling technique, the former one may be referred to as the SV-type integral equation of transfer that deals with both surface and volumetric integrals, and the latter one as the S-type integral equation of transfer. It has been demonstrated that the application of the S-type integral equation of transfer to various coordinate systems is straightforward, and it may be highly efficient in computation for multidimensional problems. It is advantageous that there is no singularity problem for the S-type equation of transfer at all locations within a participating medium.

Since the S-type integral equation method conceptually traces all rays of radiation propagating from bounding surface to a

Received Oct. 10, 1994; revision received April 28, 1995; accepted for publication July 5, 1995. 

*Associate Professor, School of Aerospace and Mechanical Engineering.

†Research Assistant, School of Aerospace and Mechanical Engineering.

point in the medium, the nonhomogeneous radiative properties may well be preserved in the formal line integral solution for intensity. In the present work, a solution method based on the S-type integral equation of transfer allowing for space-dependent radiative properties is developed, and analysis for radiation in a nonhomogeneous absorbing, emitting, and anisotropic-scattering medium with two-dimensional axisymmetric cylindrical geometry is performed. To validate the accuracy and efficiency of the current method, the PIM scheme[11] based on the SV-type integral equation of transfer is also used for the problem. The latter method is selected as a benchmark comparison because its accuracy has been documented.[10,11]

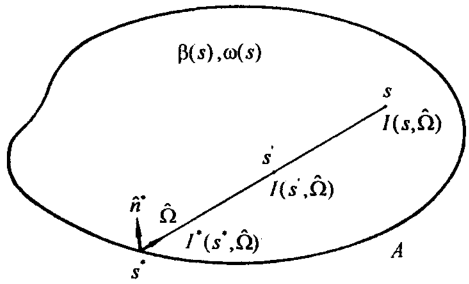

**Fig. 1 Physical model of radiative transfer in an enclosure.**

## Analysis

### S-Type Integral Equation of Transfer

For an absorbing, emitting, and scattering medium as shown in Fig. 1, the governing equation of the intensity field is

$$\frac{1}{\beta}\frac{\mathrm{d}I(s, \hat{\Omega})}{\mathrm{d}s} + I(s, \hat{\Omega}) = S(s, \hat{\Omega}) \tag{1}$$

where the source function is specified as

$$S(s, \hat{\Omega}) = (1 - \omega)I_b(s) + \frac{\omega}{4\pi}\int_{4\pi} \Phi(\hat{\Omega}, \hat{\Omega}')I(s, \hat{\Omega}')\,\mathrm{d}\Omega' \tag{2}$$

Equation (1) can be formally integrated by using an integrating factor to yield

$$I(s, \hat{\Omega}) = I^*(s^*, \hat{\Omega})\exp\left(-\int_{s^*}^{s} \beta\,\mathrm{d}s'\right) + \int_{s^*}^{s} S(s', \hat{\Omega})\exp\left(-\int_{s'}^{s} \beta\,\mathrm{d}s''\right)\beta\,\mathrm{d}s' \tag{3}$$

With the formal solution for the intensity that accounts for effects of entering intensity on boundary, emission power, and in-scattering in the medium, the incident radiation and net heat flux may be defined by the integrals related to bounding surface as

$$G(s) = \int_A I(s, \hat{\Omega})\frac{\cos(\hat{n}^*, \hat{\Omega})}{d^2(s, s^*)}\,\mathrm{d}A \tag{4}$$

$$\boldsymbol{q}(s) = \int_A I(s, \hat{\Omega})\frac{\cos(\hat{n}^*, \hat{\Omega})}{d^2(s, s^*)}\hat{\Omega}\,\mathrm{d}A \tag{5}$$

where $\hat{\Omega}$ designates a unit vector pointed from $s^*$ to $s$; $d$ denotes the distance between $s^*$ and $s$ that are located on boundary $A$ and in the radiative medium, respectively. Substituting the formal solution of the intensity $I(s, \hat{\Omega})$ given in Eq. (3) into Eqs. (4) and (5) leads to

$$G(s) = \int_A \left[I^*(s^*, \hat{\Omega})\exp\left(-\int_{s^*}^{s} \beta\,\mathrm{d}s'\right) + \int_{s^*}^{s} S(s', \hat{\Omega})\exp\left(-\int_{s'}^{s} \beta\,\mathrm{d}s''\right)\beta\,\mathrm{d}s'\right]\frac{\cos(\hat{n}^*, \hat{\Omega})}{d^2(s, s^*)}\,\mathrm{d}A \tag{6}$$

$$\boldsymbol{q}(s) = \int_A \left[I^*(s^*, \hat{\Omega})\exp\left(-\int_{s^*}^{s} \beta\,\mathrm{d}s'\right) + \int_{s^*}^{s} S(s', \hat{\Omega})\exp\left(-\int_{s'}^{s} \beta\,\mathrm{d}s''\right)\beta\,\mathrm{d}s'\right]\frac{\cos(\hat{n}^*, \hat{\Omega})}{d^2(s, s^*)}\hat{\Omega}\,\mathrm{d}A \tag{7}$$

The entering intensity, contributed by the wall emission and reflection, is expressed as

$$I^*(s^*, \hat{\Omega}) = \varepsilon I_b(s^*) + \rho^s I(s^*, \hat{\Omega}^s) + \frac{\rho^d}{\pi}\boldsymbol{q}_{\mathrm{out}}(s^*)\cdot(-\hat{n}^*) \tag{8}$$

where $\hat{\Omega}^s$ designates the specular direction into which a ray of intensity must travel after being reflected on the bounding surface from incident direction $\hat{\Omega}$.

The normal component of outgoing heat flux may be determined in terms of Eq. (7), i.e.,

$$\boldsymbol{q}_{\mathrm{out}}(s^*)\cdot(-\hat{n}^*) = \int_A \left[I^*(s^{*\prime}, \hat{\Omega}')\exp\left(-\int_{s^{*\prime}}^{s^*} \beta\,\mathrm{d}s'\right) + \int_{s^{*\prime}}^{s^*} S(s', \hat{\Omega}')\exp\left(-\int_{s'}^{s^*} \beta\,\mathrm{d}s''\right)\beta\,\mathrm{d}s'\right] \times \frac{\cos(\hat{n}^{*\prime}, \hat{\Omega}')}{d^2(s^*, s^{*\prime})}\cos(\hat{\Omega}', -\hat{n}^*)\,\mathrm{d}A' \tag{9}$$

where both points $s^{*\prime}$ and $s^*$ are located on the bounding surface $A$, $\hat{\Omega}'$ refers to the direction pointed from $s^{*\prime}$ to $s^*$ and satisfies that $\hat{\Omega}'\cdot\hat{n}^* < 0$. Note that $\boldsymbol{q}_{\mathrm{out}}(s^*)$ is the radiative heat flux irradiated from the medium onto the boundary at $s^*$.

The scattering phase function in Eq. (2) may be expressed in terms of Legendre polynomials,[16] i.e.,

$$\Phi(\hat{\Omega}, \hat{\Omega}') = 1 + \sum_{k=1}^{N} a_k P_k(\cos\Theta) \tag{10}$$

where $\cos\Theta = \hat{\Omega}\cdot\hat{\Omega}'$. The number of terms required in the expansion to simulate the phase function depends on the size of the scattering particle and the complex index of refraction. Although the current model can handle a higher order of anisotropy, here it is assumed that the scattering is linearly anisotropic, with the phase function

$$\Phi(\hat{\Omega}, \hat{\Omega}') = 1 + a_1\cos\Theta \tag{11}$$

Substituting the phase function approximation into the radiative source expression given in Eq. (2) leads to

$$S(s, \hat{\Omega}) = (1 - \omega)I_b(s) + (\omega/4\pi)[G(s) + a_1\hat{\Omega}\cdot\boldsymbol{q}(s)] \tag{12}$$

Equations (6) and (7) together with the source function expression form the S-type integral equation of transfer. Unlike the SV-type equation of transfer, the current formulations will not suffer from internal integral singularities. In the determination of $\boldsymbol{q}_{\mathrm{out}}(s^*)$, however, a singularity is established as the point $s^{*\prime}$ tends to $s^*$ on a piece of concavely curved bounding surface relative to the medium. In this case, a partition method with quadrature[11] can be used to avoid the singularity point. If $s^*$ is located on a plain or convexly curved boundary, the problem can be solved simply by extracting this area from the integral limit $A$ in Eq. (9) since any other point on the boundary cannot be seen from this point.

**Governing Equations for a Two-Dimensional Cylindrical Medium**

The general S-type integral equation of transfer expressed in Eqs. (6–9) can be readily applied for various coordinate systems. To specialize the geometry, only the direction cosines and position coordinates need to be further formulated in the equation of transfer.

For the two-dimensional, axisymmetric cylindrical medium as depicted in Fig. 2, the incident radiation and two components of net heat flux, which now is defined as $\boldsymbol{q}(r, z) = q_r(r, z)\hat{\boldsymbol{n}}_r + q_z(r, z)\hat{\boldsymbol{n}}_z$, are expressed as follows:

$$G(r, z) = 2\int_{r^*=0}^{R}\int_{\phi=0}^{\pi}\left[I(r, z, r^*, \phi, 0)\frac{z}{d^3(r, r^*, z, \phi)} + I(r, z, r^*, \phi, L)\frac{L - z}{d^3(r, r^*, z - L, \phi)}\right] r^*\,\mathrm{d}r^*\,\mathrm{d}\phi + 2\int_{z^*=0}^{L}\int_{\phi=0}^{\pi} I(r, z, R, \phi, z^*)\frac{R - r\cos\phi}{d^3(r, R, z - z^*, \phi)} \times R\,\mathrm{d}\phi\,\mathrm{d}z^* \quad \text{for } 0 \le r < R, \quad 0 < z < L \tag{13}$$

$$q_r(r, z) = 2\int_{r^*=0}^{R}\int_{\phi=0}^{\pi}\left[I(r, z, r^*, \phi, 0)\frac{z}{d^4(r, r^*, z, \phi)} + I(r, z, r^*, \phi, L)\frac{L - z}{d^4(r, r^*, z - L, \phi)}\right] \times (r - r^*\cos\phi) r^*\,\mathrm{d}r^*\,\mathrm{d}\phi + 2\int_{z^*=0}^{L}\int_{\phi=0}^{\pi} I(r, z, R, \phi, z^*) \times \frac{(R - r\cos\phi)(r - R\cos\phi)}{d^4(r, R, z - z^*, \phi)} R\,\mathrm{d}\phi\,\mathrm{d}z^* \quad \text{for } 0 \le r < R, \quad 0 \le z \le L \tag{14}$$

$$q_z(r, z) = 2\int_{r^*=0}^{R}\int_{\phi=0}^{\pi}\left[I(r, z, r^*, \phi, 0)\frac{z^2}{d^4(r, r^*, z, \phi)} - I(r, z, r^*, \phi, L)\frac{(L - z)^2}{d^4(r, r^*, z - L, \phi)}\right] r^*\,\mathrm{d}r^*\,\mathrm{d}\phi + 2\int_{z^*=0}^{L}\int_{\phi=0}^{\pi} I(r, z, R, \phi, z^*)\frac{(R - r\cos\phi)(z - z^*)}{d^4(r, R, z - z^*, \phi)} \times R\,\mathrm{d}\phi\,\mathrm{d}z^* \quad \text{for } 0 \le r \le R, \quad 0 < z < L \tag{15}$$

where the distance measured from point $(r^*, \phi, z^*)$ to point $(r, 0, z)$ is specified as

$$d(r, r^*, z - z^*, \phi) = \sqrt{r^2 + (r^*)^2 + (z - z^*)^2 - 2rr^*\cos\phi} \tag{16}$$

and the intensity at location $(r, 0, z)$, to which the ray of intensity travels from the point $(r^*, \phi, z^*)$ on boundary, may be obtained as

$$I(r, z, r^*, \phi, z^*) = I^*(r^*, \phi, z^*) \times \exp\left[-\int_{s=0}^{d(r,r^*,z-z^*,\phi)} \beta(r_s, z_s)\,\mathrm{d}s\right] + \int_{s=0}^{d(r,r^*,z-z^*,\phi)} S(r_s, \phi_s, z_s, r^*, \phi, z^*) \times \exp\left[-\int_{s'=s}^{d(r,r^*,z-z^*,\phi)} \beta(r_s', z_s')\,\mathrm{d}s'\right] \beta(r_s, z_s)\,\mathrm{d}s \tag{17}$$

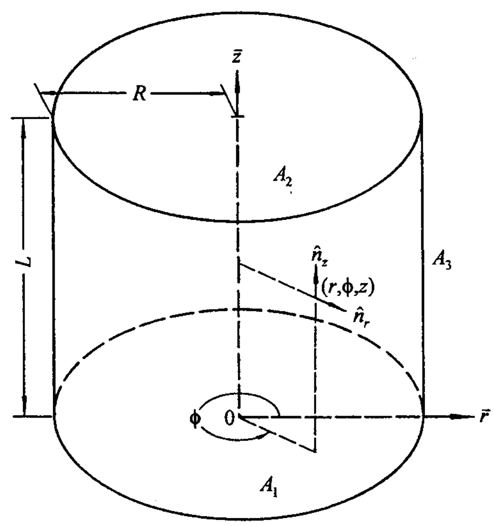


**Fig. 2 Coordinate system used in the analysis.**

where the source function is

$$S(r_s, \phi_s, z_s, r^*, \phi, z^*) = [1 - \omega(r_s, z_s)]I_b(r_s, z_s) + \frac{\omega(r_s, z_s)}{4\pi}\{G(r_s, z_s) + a_1[\cos(\hat{\boldsymbol{n}}_r, \hat{\boldsymbol{\Omega}})q_r(r_s, z_s) + \cos(\hat{\boldsymbol{n}}_z, \hat{\boldsymbol{\Omega}})q_z(r_s, z_s)]\} \tag{18}$$

The position coordinates $(r_s, \phi_s, z_s)$ are formulated as

$$r_s(s) = \sqrt{(r^*)^2 - 2sr^*\frac{r^* - r\cos\phi}{d(r, r^*, z - z^*, \phi)} + s^2\frac{d^2(r, r^*, 0, \phi)}{d^2(r, r^*, z - z^*, \phi)}} \tag{19a}$$

$$\phi_s = \phi - \cos^{-1}\left\{\frac{r_s^2 + (r^*)^2 - [sd(r, r^*, 0, \phi)/d(r, r^*, z - z^*, \phi)]^2}{2r_s r^*}\right\} \tag{19b}$$

with $\phi_s = \phi$ at $r = 0$ and

$$z_s(s) = z^* - s\frac{z^* - z}{d(r, r^*, z - z^*, \phi)} \tag{19c}$$

To avoid introducing singularity, the direction cosines in Eq. (18) are formulated as

$$\cos(\hat{\boldsymbol{n}}_r, \hat{\boldsymbol{\Omega}}) = \begin{cases} \dfrac{r^* - r\cos\phi}{d(r, r^*, z - z^*, \phi)} & \text{for } s = 0 \\ \dfrac{r_s^2 + s^2 - (r^*)^2 - (z^* - z_s)^2}{2sr_s} & \text{for } 0 < s \le d \end{cases} \tag{20}$$

$$\cos(\hat{\boldsymbol{n}}_z, \hat{\boldsymbol{\Omega}}) = \frac{z - z^*}{d(r, r^*, z - z^*, \phi)} \tag{21}$$

The entering intensities at the three bounding surfaces, considering only diffuse reflection, are specified by

$$I^*(r^*, \phi, 0) = \varepsilon I_b(r^*, 0) + (\rho^d/\pi)q_{z,\mathrm{out}}(r^*, 0) \tag{22a}$$

$$I^*(r^*, \phi, L) = \varepsilon I_b(r^*, L) + (\rho^d/\pi)q_{z,\mathrm{out}}(r^*, L) \tag{22b}$$

$$I^*(R, \phi, z^*) = \varepsilon I_b(R, z^*) + (\rho^d/\pi)q_{r,\mathrm{out}}(R, z^*) \tag{22c}$$

where $q_{r,\mathrm{out}}(R, z^*)$, $q_{z,\mathrm{out}}(r^*, 0)$, and $q_{z,\mathrm{out}}(r^*, L)$ are the normal components of heat flux irradiated from the medium into the corresponding walls. The quantity of $q_{r,\mathrm{out}}(R, z^*)$ can be evaluated by substituting $r = R$ and $z = z^*$ into Eq. (14); $q_{z,\mathrm{out}}(r^*, 0)$ and $q_{z,\mathrm{out}}(r^*, L)$ can be obtained by letting $r = r^*$, $z = 0$, and $z = L$ in Eq. (15), respectively.

**Method of Solution**

The integrations related to bounding surfaces in the governing equation for the incident radiation and heat flux can be evaluated by quadrature schemes. For the convenience of data presentation, the extended Simpson rule with equal interval of grid points is preferred for the integrations with respect to $r$ and $z$ variables, whereas the Gauss quadrature is chosen for the integrations with respect to $\phi$ because of its simple formulation and necessity to avoid a singularity point in the determination of outgoing heat flux $q_{r,\mathrm{out}}(R, z^*)$ in Eqs. (22), as noted earlier. The integrals in Eq. (17) for determining the intensity at a grid point under consideration are also directly integrated by the Gauss quadrature in this work. It leads

$$I(r, r^*, z - z^*, \phi) = I^*(r, z, r^*, \phi, z^*)\exp(-\tau^*) + \frac{d(r, r^*, z - z^*, \phi)}{2} \sum_{m=1}^{M} w_m \Lambda[d(r, r^*, z - z^*, \phi)(1 + x_m)/2] \tag{23}$$

where $\Lambda(s)$ is defined as

$$\Lambda(s) = S[r_s(s), \phi_s(s), z_s(s), r^*, \phi, z^*]\exp(-\tau)\beta(r_s, z_s) \tag{24}$$

Similarly,

$$\tau^* = \frac{d(r, r^*, z - z^*, \phi)}{2} \sum_{m=1}^{M} w_m \beta[r_s(s), z_s(s)] \tag{25}$$

$$\tau = \frac{d(r, r_s, z - z_s, \phi) - s}{2} \sum_{m=1}^{M} w_m \beta[r_s'(s'), z_s'(s')] \tag{26}$$

where $s$ and $s'$ are specified as

$$s = d(r, r^*, z - z^*, \phi)(1 + x_m)/2 \tag{27}$$

$$s' = [d(r, r_s, z - z_s, \phi) - s](1 + x_m)/2 + s \tag{28}$$

respectively.

Usually the intermediate points $(r_s, z_s)$ are not located exactly on grid points; the radiative source function at these points needs to be evaluated by interpolation in terms of the incident radiation and heat flux values at the neighboring grid points. Thus, by means of the iterative scheme such as that used in Ref. 15, the solutions of the incident radiation and heat fluxes may be obtained simultaneously.

## Results and Discussion

Numerical analysis was carried out for the test problem of radiative transfer in a two-dimensional axisymmetric cylindrical medium with prescribed distributions of emission intensity, boundary conditions, and space-dependent radiative properties.

The calculation begins with the initial guess for source function, assuming that there is no scattering effect in the radiative medium. Then, for each iteration, the source function is updated in terms of improved approximate values of entering intensity, incident radiation, and net heat fluxes at each grid point. It is observed that the incident radiation and heat fluxes converge at approximately the same rate and, therefore, the convergence criterion in the computation is chosen as $\max|G^{n+1} - G^n| < 10^{-5}$, where $n$ denotes the $n$th iteration. For all the cases considered, there is no convergence problem for the current scheme.

The numerical errors for the current method may be controlled by selecting suitable quadrature schemes and the total number of grid points. Conceptually, the finer mesh yields smaller computational error in the linear interpolation for source function at intermediate points, which usually are not located exactly on any grid point. However, as shown in Table 1, the converged solutions of incident radiation and heat fluxes are fairly insensitive to the number of total grid points as it increases from 11 × 11 to 41 × 41. The maximum relative errors of the solutions between the two grid schemes are less than 1%. For $N = 31$ and 41 the first three significant digits of these solutions become identical; therefore, the grid scheme of 31 × 31 is chosen for all following cases.

In the numerical analysis, a 20-point Gauss quadrature is used for integrations with respect to $\phi$. To determine the intensity formulated in Eq. (23), a 4-point Gauss quadrature (i.e., $M = 4$) is adopted. Accuracy has been assured by testing with higher-order Gauss quadrature schemes and the converged solution does not change significantly. The ability to use a low-order Gauss quadrature for intensity in Eq. (23) to handle the emission and scattering source contributions in the radiative medium, while maintaining a high degree of accu-

**Table 1 Convergence of incident radiation and radiative heat fluxes for an absorbing, emitting, and scattering cylindrical medium with $I_b(\tau_r, \tau_z) = 1$ and bounded by cold black walls, $\tau_R = \tau_L = 1$, $N_r = N_z = N$**

| | $G(\tau_r, 0.5)$ | | | $q_r(\tau_r, 0.5)$ | | | $q_z(\tau_r, 1.0)$ | | |
|---|---|---|---|---|---|---|---|---|---|
| $N$ | 0.0 | $\tau_r = 0.5$ | 1.0 | 0.0 | $\tau_r = 0.5$ | 1.0 | 0.0 | $\tau_r = 0.5$ | 1.0 |
| | | | | $\omega = 0.5$ | | | | | |
| 11 | 4.7886 | 4.4348 | 2.1549 | 0.0000 | 0.4224 | 1.3021 | 1.4073 | 1.3021 | 0.6322 |
| 21 | 4.7992 | 4.4450 | 2.1592 | 0.0000 | 0.4230 | 1.2917 | 1.4131 | 1.3076 | 0.6354 |
| 31 | 4.8017 | 4.4473 | 2.1614 | 0.0000 | 0.4231 | 1.2926 | 1.4149 | 1.3094 | 0.6363 |
| 41 | 4.8022 | 4.4478 | 2.1619 | 0.0000 | 0.4232 | 1.2929 | 1.4152 | 1.3097 | 0.6365 |
| | | | | $\omega = 1 - 0.75\tau_r$ | | | | | |
| 11 | 3.1437 | 3.9018 | 2.4577 | 0.0000 | 0.0519 | 1.3852 | 0.8931 | 1.1359 | 0.7278 |
| 21 | 3.1545 | 3.9122 | 2.4585 | 0.0000 | 0.0533 | 1.3881 | 0.8979 | 1.1414 | 0.7305 |
| 31 | 3.1570 | 3.9145 | 2.4603 | 0.0000 | 0.0536 | 1.3888 | 0.8992 | 1.1432 | 0.7313 |
| 41 | 3.1576 | 3.9151 | 2.4605 | 0.0000 | 0.0537 | 1.3890 | 0.8995 | 1.1435 | 0.7314 |
| | | | | $\omega = 0.375\tau_r + 0.5\tau_r^2$ | | | | | |
| 11 | 6.1403 | 4.9808 | 1.6541 | 0.0000 | 0.7960 | 1.1099 | 1.8564 | 1.4801 | 0.4771 |
| 21 | 6.1507 | 4.9947 | 1.6632 | 0.0000 | 0.7950 | 1.1157 | 1.8599 | 1.4862 | 0.4806 |
| 31 | 6.1534 | 4.9977 | 1.6657 | 0.0000 | 0.7947 | 1.1170 | 1.8608 | 1.4880 | 0.4816 |
| 41 | 6.1538 | 4.9984 | 1.6665 | 0.0000 | 0.7948 | 1.1174 | 1.8609 | 1.4883 | 0.4818 |

racy, is one of the reasons that the method is computationally efficient. The insensitivity of the converged solution to mesh fineness makes the current method preferable for use in combined radiation and conduction/convection problems, so that different resolution grid schemes may be chosen for solving the radiative transfer equation and the energy equation.

To validate the current computation code against known results from the PIM based on the SV-type integral equation of transfer,[11] several cases of radiation in an emitting, absorbing, and isotropic-scattering medium bounded by cold black walls were investigated, where the normalized emission intensity $I_b(\tau_r, \tau_z) = 1$; the extinction coefficient is maintained uniform for the entire medium, while the single scattering albedo has three variations, i.e., $\omega_1 = 0.5$, $\omega_2 = 1 - 0.75(\tau_r/\tau_R)$, $\omega_3 = 0.375(\tau_r/\tau_R) + 0.5(\tau_r/\tau_R)^2$. The latter two variable scattering coefficients are selected such that their volumetric mean values are equal to $\omega_1 = 0.5$. In Fig. 3, the heat fluxes on cylindrical and end surfaces are compared with the predictions from the PIM scheme. For all three variations of scattering albedo and two optical dimensions, the accuracy of current method is very satisfactory. The effect of variable scattering albedo on the distributions of incident radiation and $r$-component heat flux in the middle region of the cylinder is illustrated in Fig. 4, which also shows excellent agreement between solutions obtained by the PIM scheme and the current method. Although both methods yield the numerical predictions with consistent accuracy for the radiation problem, the PIM scheme consumes 1.0–2.5 × $10^4$ s for all the cases considered using a Sun SPARC-10 workstation, which is approximately 20 times the computation time required by the present modeling technique, and it also needs more programming effort.

In Fig. 5, representative results obtained by the current method are presented for the radiation in a participating me-

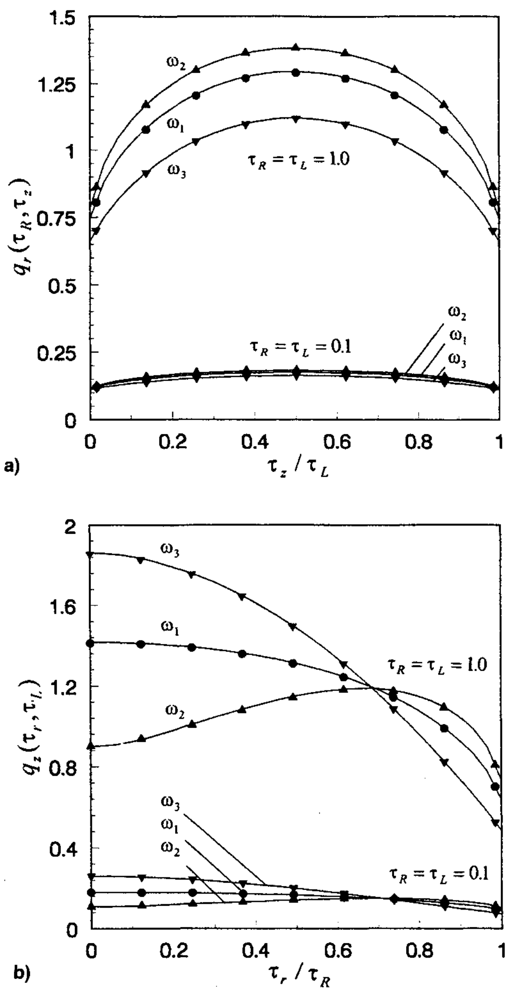


**Fig. 3 Comparison of the local wall heat fluxes a) $q_r(\tau_R, \tau_z)$ and b) $q_z(\tau_r, \tau_L)$ for the emitting, absorbing, and isotropic-scattering medium bounded by cold black walls (solid points are for PIM[11] and lines are for the current method), $I_b(\tau_r, \tau_z) = 1$, $\omega_1 = 0.5$, $\omega_2 = 1 - 0.75(\tau_r/\tau_R)$, $\omega_3 = 0.375(\tau_r/\tau_R) + 0.5(\tau_r/\tau_R)^2$.**

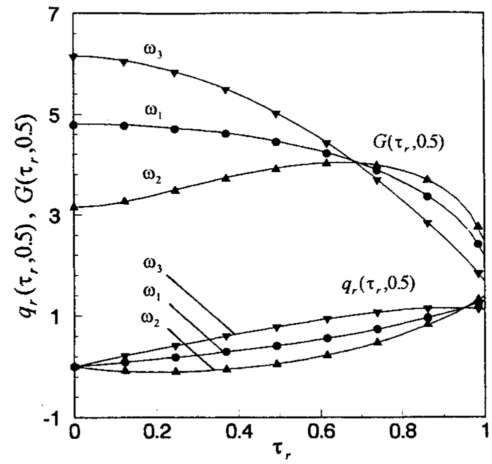


**Fig. 4 Comparison of the incident radiation $G(\tau_r, 0.5)$ and $r$-component heat flux $q_r(\tau_r, 0.5)$ for the emitting, absorbing, and isotropic-scattering medium bounded by cold black walls (solid points are for PIM[11] and lines are for the current method), $I_b(\tau_r, \tau_z) = 1$, $\tau_R = \tau_L = 1$, $\omega_1 = 0.5$, $\omega_2 = 1 - 0.75\tau_r$, $\omega_3 = 0.375\tau_r + 0.5\tau_r^2$.**

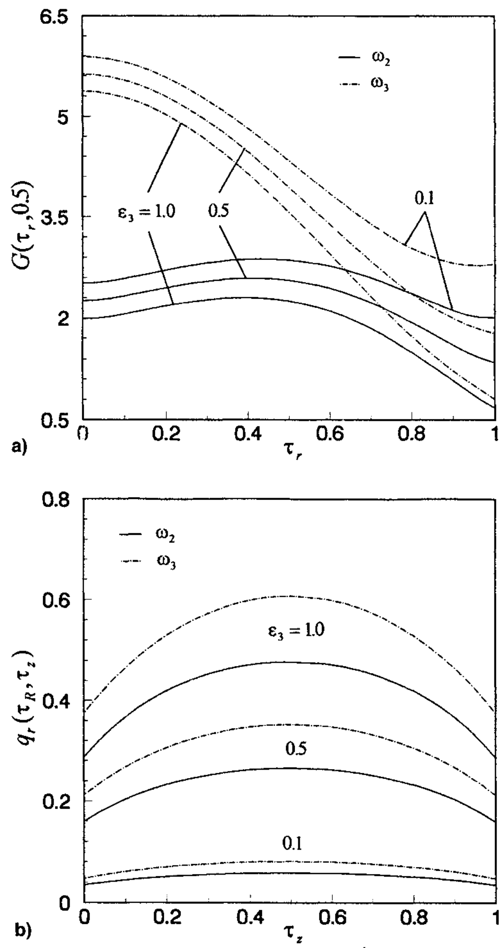


**Fig. 5 Effect of wall emissivity $\varepsilon_3$ on a) incident radiation $G(\tau_r, 0.5)$ and b) local wall heat flux $q_r(\tau_R, \tau_z)$, $I_b(\tau_r, \tau_z) = 1 - \tau_r^2$, $I_{b1}(\tau_r) = I_{b2}(\tau_r) = I_{b3}(\tau_z) = 0$, $\varepsilon_1 = \varepsilon_2 = 1$, $\tau_R = \tau_L = 1$, $\omega_2 = 1 - 0.75\tau_r$, $\omega_3 = 0.375\tau_r + 0.5\tau_r^2$.**

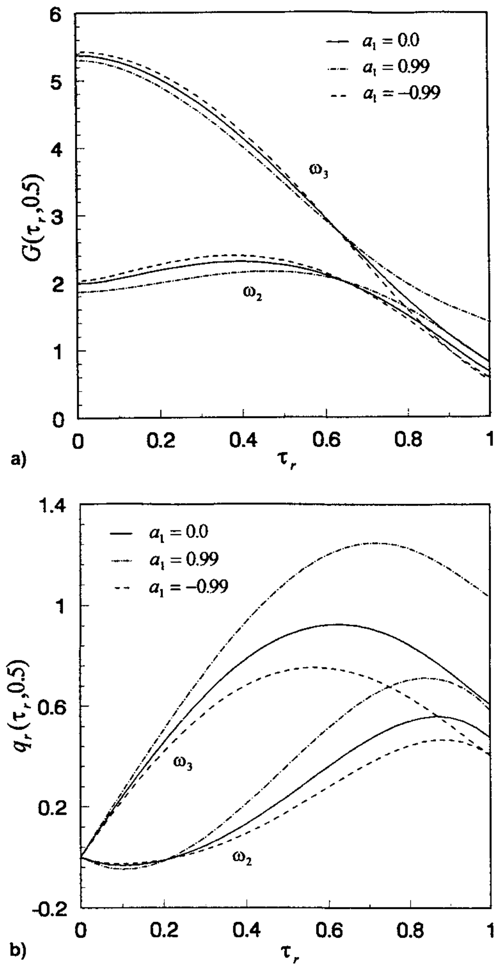


Fig. 6 Effect of linear anisotropic-scattering coefficient on a) incident radiation $G(\tau_r, 0.5)$ and b) heat flux $q_r(\tau_r, 0.5)$, $I_b(\tau_r, \tau_z) = 1 - \tau_r^2$, $I_{b1}(\tau_r) = I_{b2}(\tau_r) = I_{b3}(\tau_z) = 0$, $\varepsilon_1 = \varepsilon_2 = \varepsilon_3 = 1$, $\tau_R = \tau_L = 1$, $\omega_2 = 1 - 0.75\tau_r$, $\omega_3 = 0.375\tau_r + 0.5\tau_r^2$.

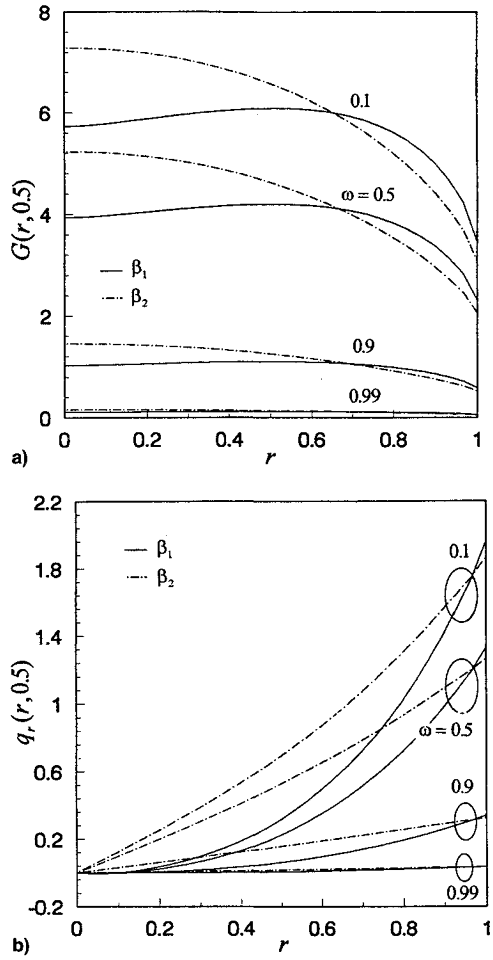


Fig. 7 Distributions of a) incident radiation $G(r, 0.5)$ and b) heat flux $q_r(r, 0.5)$ for the emitting, absorbing, and isotropic-scattering medium bounded by cold black walls, $I_b(r, z) = 1$, $R = L = 1$, $\beta_1 = 0.5 + 0.75r$, $\beta_2 = 1.2 - 0.4r^2$.

dium with isotropic scattering and normalized emission intensity $I_b(\tau_r, \tau_z) = 1 - \tau_r^2$. As expected, decreasing emissivity (in this case, the emissivity of the cylindrical wall) results in a more uniform incident radiation and heat flux distributions. It can be seen that the changes in wall emissivity $\varepsilon_3$ may affect incident radiation and heat flux on the same order as the variation of scattering property does. Therefore, to make accurate predictions for radiative transfer in the medium, both of the wall emissivities and radiative properties need to be specified with equal care.

The effect of linear anisotropic scattering coefficient on the incident radiation $G(\tau_r, 0.5)$ and heat flux $q_r(\tau_r, 0.5)$ is demonstrated in Fig. 6. With $a_1$ varying from 0.99 to $-0.99$, the incident radiation and heat flux in the core of cylindrical medium deviate relatively little from values for the isotropic scattering case, and in the region near the periphery, more dramatic variations of these quantities are observed due to stronger heat flux distribution. It is noted from the functional forms of scattering albedo variation that $\omega_3$ presents a stronger scattering effect than the $\omega_2$ case as $r \to R$, and so the impact of the anisotropic scattering for the $\omega_3$ case is more obvious near a cylindrical surface.

For the previously considered cases, the extinction coefficient is specified as a constant for simplicity. However, for most practical applications, nonhomogeneity in the extinction coefficient (because of absorption) is much more likely than the albedo variation. In Fig. 7 the distributions of incident radiation $G(r, 0.5)$ and $r$-component heat flux $q_r(r, 0.5)$ are presented for an emitting, absorbing, and isotropic-scattering medium bounded by cold black walls. The emission source and two cases ($\beta_1$ and $\beta_2$) of variable extinction coefficient are assumed as $I_b(r, z) = 1$, $\beta_1 = 0.5 + 0.75r$, and $\beta_2 = 1.2 - 0.4r^2$. For the absorption-dominant situation (i.e., small single scattering albedo), the variable extinction coefficient has a more obvious effect on the incident radiation and heat flux, whereas for the strong scattering case its effect becomes insignificant because of the negligible contribution of the emitting source, especially as single-scattering albedo approach unity.

## Conclusions

The S-type integral equation of radiative transfer is generalized to allow for space-dependent radiative properties in a participating medium. The model is subsequently applied to a two-dimensional axisymmetric cylindrical geometry. The numerical analysis performed for the test problem shows that the method can be successfully used for accurate predictions of radiative transfer in both homogeneous and nonhomogeneous media and the solution scheme based on it is accurate, simple, and computationally efficient.

## Acknowledgment

This work was sponsored in part by U.S. Department of Energy Contract DE-FG22-94BC 14971.

## References

[1]Modest, M. F., "Modified Differential Approximation for Radiative Transfer in General Three-Dimensional Media," *Journal of*

*Thermophysics and Heat Transfer*, Vol. 3, No. 3, 1989, pp. 283–288.
[2]Thynell, S. T., "Treatment of Radiation Heat Transfer in Absorbing, Emitting, Scattering, Two-Dimensional Cylindrical Media," *Numerical Heat Transfer*, Pt. A, Vol. 17, 1990, pp. 449–472.
[3]Wu, C.-Y., "Radiative Transfer in a Rectangular Anisotropically Scattering Medium Exposed to Diffuse Radiation," *Journal of Quantitative Spectroscopy & Radiative Transfer*, Vol. 43, No. 3, 1990, pp. 217–224.
[4]Yuen, W. W., and Takara, E. E., "Superposition Technique for Radiative Equilibrium in Rectangular Enclosures with Complex Boundary Conditions," *International Journal of Heat and Mass Transfer*, Vol. 33, No. 5, 1990, pp. 901–915.
[5]Tan, Z., and Howell, J. R., "New Numerical Method for Radiation Heat Transfer in Nonhomogeneous Participating Media," *Journal of Thermophysics and Heat Transfer*, Vol. 4, No. 4, 1990, pp. 419–424.
[6]Walters, D. V., and Buckius, R. O., "Mean Emission Length Approach to Multidimensional Radiative Transfer Including Scattering and Real Gas Absorption," *International Journal of Heat and Mass Transfer*, Vol. 35, No. 1, 1992, pp. 131–140.
[7]Farmer, J. T., and Howell, J. R., "Monte Carlo Solution of Radiative Heat Transfer in a Three-Dimensional Enclosure with an Anisotropically Scattering, Spectrally Dependent, Inhomogeneous Medium," Vol. 203, ASME-HTD, 1992, pp. 301–309.
[8]Walters, D. V., and Buckius, R. O., "Rigorous Development for Radiation Heat Transfer in Nonhomogeneous Absorbing, Emitting and Scattering Media," *International Journal of Heat and Mass Transfer*, Vol. 35, No. 12, 1992, pp. 3323–3333.
[9]Jendoubi, S., Lee, H. S., and Kim, T.-K., "Discrete Ordinates Solutions for Radiatively Participating Media in a Cylindrical Enclosure," *Journal of Thermophysics and Heat Transfer*, Vol. 7, No. 2, 1993, pp. 213–219.
[10]Tan, Z., "Radiative Heat Transfer in Multidimensional Emitting, Absorbing, and Anisotropic Scattering Media—Mathematical Formulation and Numerical Method," *Journal of Heat Transfer*, Vol. 111, No. 1, 1989, pp. 141–147.
[11]Zhang, J.-M., and Sutton, W. H., "Multidimensional Radiative Transfer in Absorbing, Emitting and Linearly Anisotropic Scattering Cylindrical Medium with Space-Dependent Properties," *Journal of Quantitative Spectroscopy & Radiative Transfer*, Vol. 52, No. 6, 1994, pp. 791–808.
[12]Lin, J.-D., "Exact Expressions for Radiative Transfer in an Arbitrary Geometry Exposed to Radiation," *Journal of Quantitative Spectroscopy & Radiative Transfer*, Vol. 37, No. 6, 1987, pp. 591–601.
[13]Thynell, S. T., "The Integral Form of the Equation of Transfer in Finite, Two-Dimensional, Cylindrical Media," *Journal of Quantitative Spectroscopy & Radiative Transfer*, Vol. 42, No. 2, 1989, pp. 117–136.
[14]Wu, C.-Y., "Exact Integral Formulation for Radiative Transfer in an Inhomogeneous Scattering Medium," *Journal of Thermophysics and Heat Transfer*, Vol. 4, No. 4, 1990, pp. 425–431.
[15]Zhang, J.-M., and Sutton, W. H., "The Source Approximation Method for Multidimensional Media Using the Surface-Integral Form of Radiative Transfer Equation," *Journal of Quantitative Spectroscopy & Radiative Transfer*, Vol. 53, No. 5, 1995, pp. 549–563.
[16]Modest, M. F., *Radiative Heat Transfer*, McGraw–Hill, New York, 1993, pp. 388–420.